Determination of the axial nucleon form factor from the MiniBooNE data

A. V. Butkevich[1] and D. Perevalov[2]

[1]*Institute for Nuclear Research, Russian Academy of Sciences,*

60th October Anniversary Prospect 7A, Moscow 117312, Russia

[2]*Fermi National Accelerator Laboratory, Batavia, Illinois 60510, USA*

(Dated: March 19, 2014)

Both neutrino and antineutrino charged-current quasielastic scattering on a carbon target are studied to investigate the nuclear effect on the determination of the axial form factor $F_A(Q^2)$. A method for extraction of $F_A(Q^2)$ from the flux-integrated $d\sigma/dQ^2$ cross section of (anti)neutrino scattering on nuclei is presented. Data from the MiniBooNE experiment are analyzed in the relativistic distorted-wave impulse approximation, the Fermi gas model, and the Fermi gas model with enhancements in the transverse cross section. We found that the values of the axial form factor, extracted in the impulse approximation and predicted by the dipole approximation with the axial mass $M_A \approx 1.37$, GeV are in good agreement. The agreement between the extracted form factor and meson-dominance ansatz also is good. On the other hand, the Q^2 dependence of F_A extracted in the approach with the transverse enhancement is found to differ significantly from the dipole approximation.

PACS numbers: 25.30.-c, 25.30.Bf, 25.30.Pt, 13.15.+g

I.   INTRODUCTION

One of the main systematic errors in the neutrino experiments are those associated with neutrino cross sections. The high-intensity neutrino beams used in neutrino oscillation experiments are peaked in the 0.3-5 GeV energy domain and allow the study of neutrino-nucleus interaction with unprecedented detail. In this energy range the dominant contribution to neutrino-nucleus scattering comes from the charged-current quasielastic (CCQE) reactions and resonance production processes.

Various modern [1–7] neutrino experiments reported measurements of the differential

$d\sigma/dQ^2$ (Q^2 is squared four-momentum transfer) [1–6], double-differential [2, 4, 7] and total cross sections [1, 2, 4, 7, 8] of CCQE scattering. This interaction represents a two-particle scattering process with lepton and nucleon in the final state. Since the criteria used to select CCQE events are strongly influenced by both target material and detector technology, various selection techniques are applied in these experiments (tracking and Cerenkov detector). In neutrino scattering experiments, the neutrino energy is unknown. However, both the neutrino energy and Q^2 can be evaluated based on the kinematics of the outgoing final state particles.

With the assumptions of conserved vector current and partially conserved axial current, the only undetermined form factor in the theoretical description of the CCQE neutrino scattering is the axial nucleon form factor. In most analysis of neutrino interaction on complex nuclei, the dipole parametrization of $F_A(Q^2)$ with one parameter, the axial mass M_A, is used. The analyses are mainly based on the relativistic Fermi gas model (RFGM) [9] and involve some additional model dependence due to nuclear structure. While constraints exist from pion electroproduction data with $M_A = 1.06 \pm 0.016$ GeV [10], neutrino experiments usually treat axial mass M_A in CCQE as independent of that measurement.

The values of M_A are obtained from a fit to observed Q^2 distribution of events, differential and total (anti)neutrino CCQE interaction cross sections. The formal averaging of M_A values which are very widely spread was done in Ref. [10]: $M_A = 1.026 \pm 0.021$ GeV. This result is also known as world-averaged value of the axial mass. Values of M_A determined from the recent QE (anti)neutrino-carbon scattering experiments range anywhere from $M_A \approx 1$ to 1.35 GeV. The NOMAD Collaboration [1] reports $M_A = 1.05 \pm 0.02 \pm 0.06$ GeV, and the most resent MINERvA [5, 6] results are consistent with $M_A \simeq 0.99$ GeV. On the other hand, the MiniBooNE Collaboration [2–4] reports a large value of $M_A = 1.35 \pm 0.17$ GeV. The other recent results [11–14] similarly find central values higher than the above-mentioned world average. The absolute values of the differential and total cross sections measured by MiniBooNE are about 30% larger as compared to the NOMAD results. It is essential to obtain consistency between experiments utilizing different beam energies, nuclear targets, and detectors.

The radius of the nucleon axial charge distribution in terms of the dipole mass is defined as $\langle r_A^2 \rangle = 12/M_A^2$, and for $1.032 \leq M_A \leq 1.35$ GeV it can be estimated as $0.51 \leq r_A \leq 0.66$ fm. So, a large value of $M_A = 1.35$ GeV corresponds to a rather small axial charge

radius of about 0.51 fm. On the other hand, the typical nucleon size as deduced from the electron scattering experiment is about 0.85 fm, whereas model-dependent analyses of proton-antiproton annihilation lead to a baryon charge radius of about 0.5 fm [10].

These results have encounraged many theoretical studies [15–29] to attempt to explain the discrepancy between the data and traditional nuclear model, i.e., the RFGM. Some models that are based on the impulse approximation lead to large value of M_A [15–18] in the MiniBooNE data. For instance, in Refs. [17, 18], a value of $M_A = 1.37$ GeV, that fits the Q^2 shape of the measured $d\sigma/dQ^2$ cross section was obtained within the RFGM, and relativistic distorted-wave impulse approximation (RDWIA) approaches.

Other nuclear models [20–24] include effects of multinucleon excitations such as meson-exchange currents (MECs) and isobar currents (ICs) to describe the MiniBooNE data. The contribution of the two-particle-two-hole (2p-2h) excitations to CCQE scattering has been found to be sizable and allows one to reproduce the MiniBooNE cross sections with value of $M_A \approx 1.03$ GeV. This result suggests that much of the cross section (about 30%) measured by the MiniBooNE experiment can be attributed to processes that are not properly QE scattering. However, fully relativistic microscopic calculations of 2p-2h contributions are extremely difficult and may be bound to model-dependent assumptions. Future theoretical work is obviously needed to improve the present models that include effects beyond the impulse approximation. The transverse enhancement (TE) effective model to account for MEC effects has been proposed in Ref. [28]. In this model, the magnetic form factors for nucleons bound in carbon are modified to describe the enhancement in the transverse electron-carbon QE cross section. The other nucleon form factors are the same as for free nucleons. It allows one to describe the MiniBooNE data (total cross section) by using the dipole approximation for $F_A(Q^2)$ with $M_A = 1.014$ GeV.

The assumption of the dipole ansatz for the axial form factor is a crucial element in these studies. The dipole parametrization of $F_A(Q^2)$ has no strict theoretical basis and the choice of this parametrization is made by analogy with electromagnetic form factors. On the other hand the dipole ansatz has been found to conflict with electron scattering data for the vector form factor [28]. A model-independent description of the axial form factor was presented in Ref. [30]. The application of analyticity and dispersion relations to the axial form factor in the RFGM to find constraints for the axial mass using the data from MiniBooNE produces the value of $M_A \approx 0.85$ GeV which differs significantly from

extractions based on the traditional dipole ansatz.

The pion and nucleon form factors were discussed in Ref. [31] within the large-N_c approach in the spacelike region. It was shown that, if the error bars on the monopole mass are taken into account one can make the dipole overlap with a product of monopoles within the corresponding error bars provided with the half-width rule. This construction is based on the following assumptions: (a) hadronic form factors in the spacelike region are dominated by mesonic states with the relevant quantum number, (b) the high-energy behavior is given by perturbative QCD, and the number of mesons is taken to be minimal to satisfy these conditions, and (c) errors in the meson-dominated form factors are estimated by means of the half-width rule.

In Ref. [32] the values of $F_A(Q^2)$ as a function of Q^2 were extracted from the differential cross section of neutrino scattering on deuterium (on a "quasifree" nucleon). A reasonable description of axial form factor by dipole approximation with $M_A = 1.014 \pm 0.016$ GeV was found. The current data on CCQE scattering come from a variety of experiments operating with carbon, oxygen, and iron data. Therefore the aim of this work is twofold. First, we propose a method which allow one to determine $F_A(Q^2)$ as a function of Q^2 directly from the measured flux-integrated $d\sigma/dQ^2$ cross section of CCQE (anti)neutrino scattering on nuclei. Second, we apply the method and extract the Q^2-dependence of the axial form factor from MiniBooNE data [2, 4] in the RFGM, RDWIA and RFGM+TE approaches and show that the Q^2-dependence for the axial and vector form factors are correlated. We also compare the extracted Q^2-dependence of $F_A(Q^2)$ with predictions of the meson-dominance ansatz and dipole approximation predictions with $M_A \approx 1$ GeV and $M_A \approx 1.3$ GeV

The outline of this paper is the following. In Sec. II we present briefly the RDWIA model and discuss the procedure which allows determination of the axial form factor from the flux-integrated $d\sigma/dQ^2$ (anti)neutrino cross section. Section III presents results of the extraction of F_A from the MiniBooNE data and calculations of the flux-unfolded total cross sections for antineutrino scattering off carbon . Our conclusions are summarized in Sec. IV.

II.   MODEL AND METHOD FOR EXTRACTION OF $F_A(Q^2)$ FROM FLUX-INTEGRATED $d\sigma/dQ^2$ DIFFERENTIAL CROSS SECTIONS

The formalism of CCQE exclusive

$$\nu(k_i) + A(p_A) \rightarrow \mu(k_f) + N(p_x) + B(p_B), \tag{1}$$

and inclusive

$$\nu(k_i) + A(p_A) \rightarrow \mu(k_f) + X \tag{2}$$

scattering off nuclei in the one-W-boson exchange approximation has been extensively described in previous works [33–36]. Here $k_i = (\varepsilon_i, \boldsymbol{k}_i)$ and $k_f = (\varepsilon_f, \boldsymbol{k}_f)$ are the initial and final lepton momenta respectively, $p_A = (\varepsilon_A, \boldsymbol{p}_A)$, and $p_B = (\varepsilon_B, \boldsymbol{p}_B)$ are the initial and final target momenta, respectively $p_x = (\varepsilon_x, \boldsymbol{p}_x)$ is the ejectile nucleon momentum, $q = (\omega, \boldsymbol{q})$ is the momentum transfer, and $Q^2 = -q^2 = \boldsymbol{q}^2 - \omega^2$.

A. Model

All the nuclear structure information and final state interaction (FSI) effects are contained in the weak CC nuclear tensors $W_{\mu\nu}$, which are given by a bilinear product of the transition matrix elements of the nuclear CC operator J_μ between the initial nucleus state and the final state. We describe CCQE neutrino-nuclear scattering in the impulse approximation (IA), assuming that the incoming neutrino interacts with only one nucleon, which is subsequently emitted, while the remaining (A-1) nucleons in the target are spectators. The nuclear current is written as the sum of single-nucleon currents.

The single-nucleon charged current has $V-A$ structure $J^\mu = J_V^\mu + J_A^\mu$. For a free-nucleon vertex function $\Gamma^\mu = \Gamma_V^\mu + \Gamma_A^\mu$ we use the vector current vertex function $\Gamma_V^\mu = F_V(Q^2)\gamma^\mu + i\sigma^{\mu\nu}q_\nu F_M(Q^2)/2m$, where $\sigma^{\mu\nu} = i[\gamma^\mu, \gamma^\nu]/2$ and F_V and F_M are the weak vector form factors. They are related to the corresponding electromagnetic ones for protons and neutrons by the hypothesis of the conserved vector current. We use the approximation of Ref. [37] on the nucleon form factors. Because the bound nucleons are off shell we employ the de Forest prescription [38] and the Coulomb gauge for off-shell vector current vertex Γ_V^μ.

The axial current vertex function can be written in terms of the axial $F_A(Q^2)$ and the pseudoscalar $F_P(Q^2)$ form factors:

$$\Gamma_A^\mu = F_A(Q^2)\gamma^\mu\gamma_5 + F_P(Q^2)q^\mu\gamma_5 \tag{3}$$

The pseudoscalar form factor $F_P(Q^2)$ is dominated by the pion pole and is given in term of the Godberger-Treiman relation near $Q^2 \approx 0$ if partially conserved axial current is assumed.

We assume that the similar relation is valid for high Q^2 as well and write

$$F_p = \frac{2m^2 F_A(Q^2)}{m_\pi^2 + Q^2} = F_A(Q^2)F'_P(Q^2), \tag{4}$$

where $F'_P(Q^2) = 2m^2/(m_\pi^2 + Q^2)$ and m_π is the pion mass. Then the axial current vertex function can be written in the form

$$\Gamma_A^\mu = F_A(Q^2)[\gamma^\mu \gamma_5 + F'_P(Q^2)q^\mu \gamma_5]. \tag{5}$$

Thus the only undetermined form factor is the axial form factor that is commonly parametrized as a dipole

$$F_A = \frac{F_A(0)}{(1 + Q^2/M_A^2)^2} \tag{6}$$

where $F_A(0)$=1.267 and M_A is the axial mass, which controls the Q^2 dependence of F_A, and ultimately, the normalization of the predicted cross section. We calculated the relativistic wave functions of the bound nucleon states in the independent particle shell model as the self-consistent solutions of a Dirac equation, derived within a relativistic mean field approach, from a Lagrangian containing σ, ω, and ρ mesons (the $\sigma - \omega$ model)[39, 40]. According to the JLab data [41, 42] the occupancy of the independent particle shell-model orbitals of ^{12}C equals on average 89%. In this work we assume that the missing strength (11%) can be attributed to the short-range nucleon-nucleon (NN) correlations in the ground state, leading to the appearance of the high-momentum and high-energy component in the nucleon distribution in the target. These estimates of the depletion of hole states follow from the RDWIA analysis of ^{12}C$(e, e'p)$ for $Q^2 < 2$ (GeV/c)^2 [42] and are consistent with a direct measurement of the spectral function [43], which observed approximately 0.6 protons in a region attributable to a single-nucleon knockout from a correlated cluster.

In the RDWIA, final state interaction effects for the outgoing nucleon are taken into account. The distorted-wave function of the knocked out nucleon is evaluated as a solution of a Dirac equation containing a phenomenological relativistic optical potential. We use the LEA program [44] for the numerical calculation of the distorted wave functions with the EDAD1 parametrization [45] of the relativistic optical potential for carbon. This code, initially designed for computing exclusive proton-nucleus and electron-nucleus scattering, was successfully tested against A$(e, e'p)$ data [41, 46], and we adopted this program for neutrino reactions.

A complex optical potential with a nonzero imaginary part generally produces an absorption of the flux. For the exclusive $A(l, l'N)$ channel this reflects the coupling between different open reaction channels. However, for the inclusive reaction, the total flux must be conserved. Therefore, we calculate the inclusive and total cross sections with the EDAD1 relativistic optical potential in which only the real part is included.

The inclusive cross sections with the FSI effects in the presence of the short-range NN correlations were calculated by using the method proposed in Refs. [33, 36]. In this approach the contribution of the NN correlated pairs is evaluated in the IA, i.e., the virtual boson couples to only one member of the NN-pair. It is one-body process that leads to the emission of two nucleons (2p-2h excitation). The contributions of the two-body currents, such as meson-exchange currents and isobar currents, are not considered.

B. Method for extraction of $F_A(Q^2)$ from flux-integrated $d\sigma/dQ^2$ cross sections

The inclusive weak hadronic tensor $W_{\mu\nu}$ is given by bilinear products of the transition matrix elements of the nuclear weak current operators J_μ between the initial and final nuclear states, i.e., $W_{\mu\nu} = \langle J_\mu J_\nu^\dagger \rangle$, where the angle brackets denote products of matrix elements, appropriately averaged over initial states and summed over final states.

By using Eq. (5), the axial vector current can be factorized in the form

$$J_A = F_A(Q^2) J_A'(Q^2), \tag{7}$$

where

$$J_A' = \gamma^\mu \gamma_5 + F_P'(Q^2) q^\mu \gamma_5, \tag{8}$$

and the weak current can be expressed as $J = J_V + F_A J_A'$. The expression for the hadronic tensor is then given by

$$W_{\mu\nu} = W_{\mu\nu}^V + F_A^2(Q^2) W_{\mu\nu}^A + h F_A(Q^2) W_{\mu\nu}^{VA}, \tag{9}$$

where $W_{\mu\nu}^V = \langle (J_V)_\mu (J_V)_\nu^\dagger \rangle$, $W_{\mu\nu}^A = \langle (J_A')_\mu (J_A')_\nu^\dagger \rangle$, $W_{\mu\nu}^{VA} = \langle (J_V)_\mu (J_A')_\nu^\dagger + (J_A')_\mu (J_V)_\nu^\dagger \rangle$, and h is 1 for a neutrino and -1 for an antineutrino. Finally, contracting $W_{\mu\nu}$ with the lepton tensor we obtain the inclusive (anti)neutrino scattering cross section $d\sigma/dQ^2$ in terms of vector σ^V, axial σ^A, and vector-axial σ^{VA} cross sections

$$\frac{d\sigma^{\nu,\,\bar\nu}}{dQ^2}(Q^2, \varepsilon_i) = \sigma^V(Q^2, \varepsilon_i) + F_A^2(Q^2) \sigma^A(Q^2, \varepsilon_i) + h F_A(Q^2) \sigma^{VA}(Q^2, \varepsilon_i), \tag{10}$$

where $\sigma^V = d\sigma/dQ^2(F_A = 0)$ and $\sigma^A = d\sigma/dQ^2(F_V = F_M = 0, F_A = 1)$. The vector (axial) cross section is due to the vector (axial) component of the weak current and it can be calculated as the $d\sigma/dQ^2$ cross section with $F_A(Q^2) = 0$ ($F_V(Q^2) = F_M(Q^2) = 0, F_A(Q^2) = 1$). So, the cross section $\sigma^A(Q^2)$ does not depend on vector form factors, i.e., on the longitudinal or transverse QE response functions. The vector-axial cross section σ^{VA}, arising from the interference between the vector and axial currents can be written as

$$\sigma^{VA} = [\sigma(F_A = 1) - \sigma^V - \sigma^A], \qquad (11)$$

where $\sigma(F_A = 1)$ is the $d\sigma/dQ^2$ cross section, calculated with $F_A(Q^2)=1$.

In the simplest case of (anti)neutrino scattering off a free nucleon the cross sections σ^V, σ^A, and σ^{VA} can be expressed in terms of the vector form factors F_V and F_M. For instance [47],

$$\sigma^{VA} = \frac{G_F^2}{2\pi} \cos^2 \theta_c \frac{Q^2}{m\varepsilon_i} \left(1 - \frac{Q^2}{4m\varepsilon_i}\right) [F_V(Q^2) + F_M(Q^2)], \qquad (12)$$

where G_F is the Fermi constant and θ_c is the Cabibbo angle. The difference

$$\frac{d\sigma^\nu}{dQ^2}(Q^2, \varepsilon_i) - \frac{d\sigma^{\bar\nu}}{dQ^2}(Q^2, \varepsilon_i) = 2F_A(Q^2)\sigma^{VA}(Q^2, \varepsilon_i), \qquad (13)$$

is going to zero at $Q^2 \to 0$ and decreases with (anti)neutrino energy.

Our RDWIA results for the σ^V, σ^A, and σ^{VA} cross sections for neutrino CCQE scattering off carbon are shown in Fig. 1 as functions of Q^2 for neutrino energies ε_ν=0.5, 0.7, 1.2, and 2.5 GeV. The cross section σ^V has a maximum at $Q^2 \approx 0.15$ (GeV/c)^2 and depends slowly on neutrino energy. The cross section σ_A is dominant at $\varepsilon_\nu > 1$ GeV in the range $Q^2 > 0.2$ (GeV/c)^2 and slowly decreases with Q^2. On the other hand, the cross section σ^{VA} decreases with neutrino energy as $\sim 1/\varepsilon_\nu$. At $\varepsilon_\nu > 1$ GeV, it depends slowly on Q^2 in the range $Q^2 > 0.3$ (GeV/c)^2.

In neutrino experiments the differential cross sections of CCQE neutrino-nucleus scattering are measured within rather wide ranges of the (anti)neutrino energy spectrum. Therefore, flux-averaged and flux-integrated differential cross sections can be extracted. The MiniBooNE ν_μ and $\bar\nu_\mu$ CCQE flux-integrated $\langle d\sigma^{\nu,\bar\nu}/dQ^2 \rangle$ cross sections were measured as functions of Q^2 in the range $0 \le Q^2 \le 2$ (GeV/c)^2 [2, 4]. These cross sections can be written as

$$\left\langle \frac{d\sigma^{\nu,\bar\nu}}{dQ^2}(Q^2) \right\rangle = \int_{\varepsilon_{min}}^{\varepsilon_{max}} W_{\nu,\bar\nu}(\varepsilon_i) \frac{d\sigma^{\nu,\bar\nu}}{dQ^2}(Q^2, \varepsilon_i) d\varepsilon_i. \qquad (14)$$
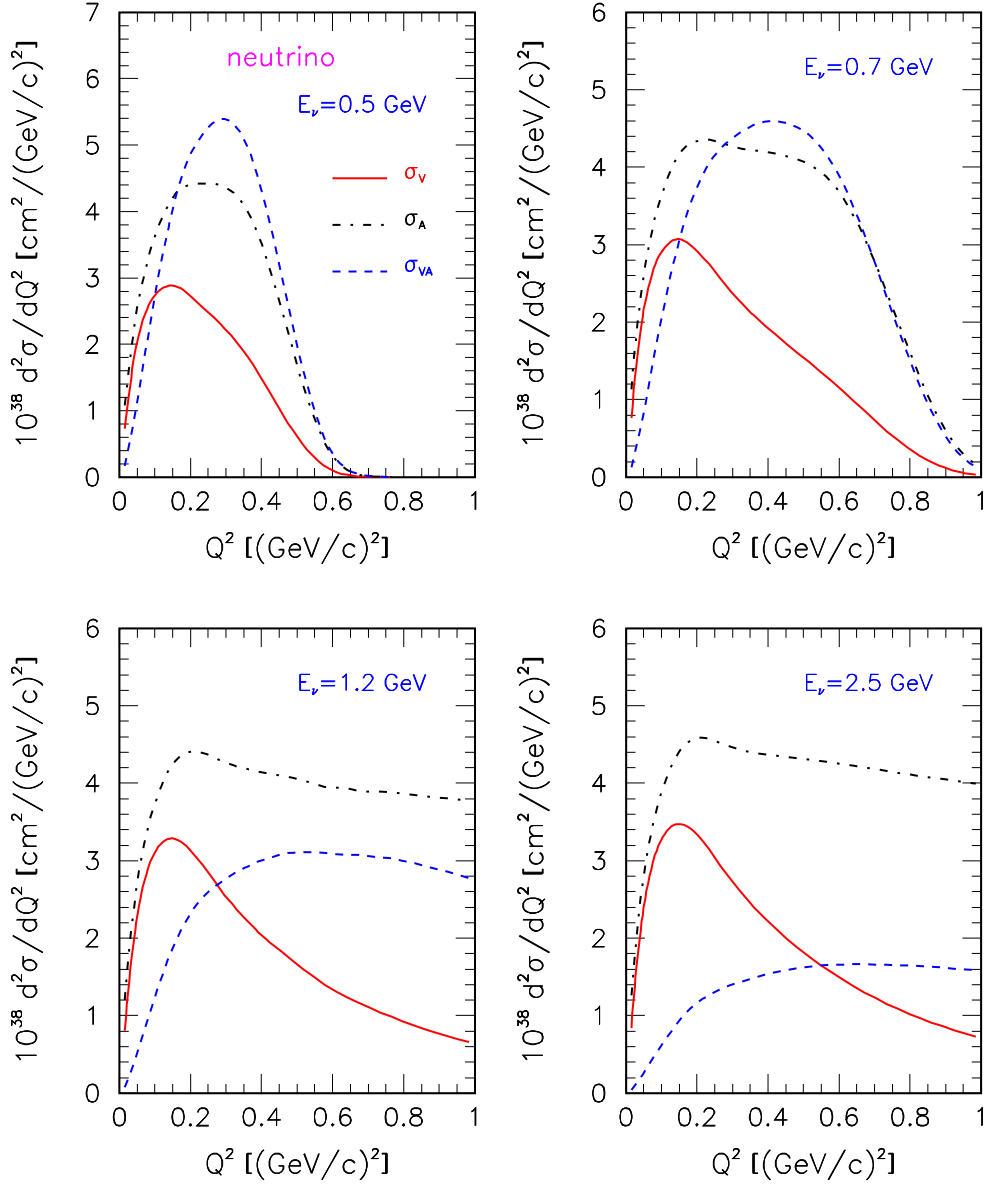
FIG. 1: (Color online) Differential cross sections σ_V (solid line), σ_A (dashed-dotted line), and σ_{VA} (dashed line) vs four-momentum transfer Q^2 for neutrino scattering off carbon calculated in the RDWIA approach for four values of incoming neutrino energy: $\varepsilon_\nu = 0.5, 0.7, 1.2$ and 2.5 GeV.

The weight functions $W_{\nu,\bar{\nu}}$ are defined as

$$W_{\nu,\bar{\nu}}(\varepsilon_i) \;=\; I_{\nu,\bar{\nu}}(\varepsilon_i)/\Phi_{\nu,\bar{\nu}}, \tag{15}$$

where $I_{\nu,\bar{\nu}}(\varepsilon_i)$ is the neutrino (antineutrino) spectrum and $\Phi_{\nu,\bar{\nu}}$ is the neutrino (antineutrino) flux in $\nu(\bar{\nu})$-beam mode [49], integrated over $0 \leq \varepsilon_i \leq 3$ GeV. Combining Eq. (10) with

Eq. (14) we obtain the flux-integrated $\langle d\sigma^{\nu,\bar{\nu}}/dQ^2 \rangle$ cross section in terms of flux-integrated $\langle \sigma^V \rangle$, $\langle \sigma^A \rangle$, and $\langle \sigma^{VA} \rangle$ cross sections

$$\left\langle \frac{d\sigma^{\nu,\bar{\nu}}}{dQ^2}(Q^2) \right\rangle = \langle \sigma^V(Q^2) \rangle^{\nu,\bar{\nu}} + F_A^2(Q^2)\langle \sigma^A(Q^2) \rangle^{\nu,\bar{\nu}} + hF_A(Q^2)\langle \sigma^{VA}(Q^2) \rangle^{\nu,\bar{\nu}}, \quad (16)$$

where

$$\langle \sigma^j(Q^2) \rangle^{\nu,\bar{\nu}} = \int_{\varepsilon_{min}}^{\varepsilon_{max}} W_{\nu,\bar{\nu}}(\varepsilon_i)[\sigma^j(Q^2,\varepsilon_i)]^{\nu,\bar{\nu}} d\varepsilon_i \quad (17)$$

are the flux-integrated vector, axial, and vector-axial ($j = V, A, AV$) cross sections. The values of $F_A(Q^2)$ can be extracted as the solution of Eq. (16), by using the data for $\langle d\sigma^{\nu,\bar{\nu}}/dQ^2 \rangle$. In the case of neutrino scattering on deuterium (quasifree nucleon) this procedure was applied in Ref. [48] for the extraction of $F_A(Q^2)$ as a function of Q^2.

Because the flux-integrated cross sections $\langle \sigma^j \rangle$ depend on the nuclear model, vector form factors, and the predicted (anti)neutrino flux, the extracted values of the axial form factor are model dependet and implicitly include the uncertainties in the F_V, F_M, and $(\bar{\nu}_\mu)\nu_\mu$ flux.

III. RESULTS AND ANALYSIS

A. CCQE flux-integrated $\langle d\sigma^i(Q^2) \rangle$ differential cross sections

The MiniBooNE $\nu_\mu(\bar{\nu}_\mu)$ CCQE flux-integrated differential cross sections $d\sigma/dQ^2$ were extracted as functions of Q^2 in the range $0 \leq Q^2 \leq 2$ (GeV/c)^2 [2, 4]. The cross sections are scaled with the number of neutron (proton) in the target. A "shape-only" fit to the cross sections was performed to extract values for adjusted CCQE model parameters, M_A and κ, within the Fermi gas model with the dipole parametrization of $F_A(Q^2)$. To tune this model to the low Q^2, the parameter κ was introduced. The "shape-only" fit yields the model parameters, $M_A = 1.35 \pm 0.17$ (GeV/c)^2 and $\kappa = 1.007 \pm 0.012$. The extracted value for M_A is approximately 30% higher than the world-averaged one. The prediction of the RFGM with these values of the parameters also describes well the measured (anti)neutrino flux-folded differential cross section $d\sigma^{\nu,\bar{\nu}}/dQ^2$.

To extract the values of the axial form factor $F_A(Q^2)$ as a function of Q^2 from the MiniBooNE neutrino and antineutrino flux-folded $d\sigma^{\nu,\bar{\nu}}/dQ^2$ cross sections we calculated the flux-integrated $\langle \sigma^V \rangle^{\nu,\bar{\nu}}$, $\langle \sigma^A \rangle^{\nu,\bar{\nu}}$, and $\langle \sigma^{VA} \rangle^{\nu,\bar{\nu}}$ cross sections with booster neutrino beam
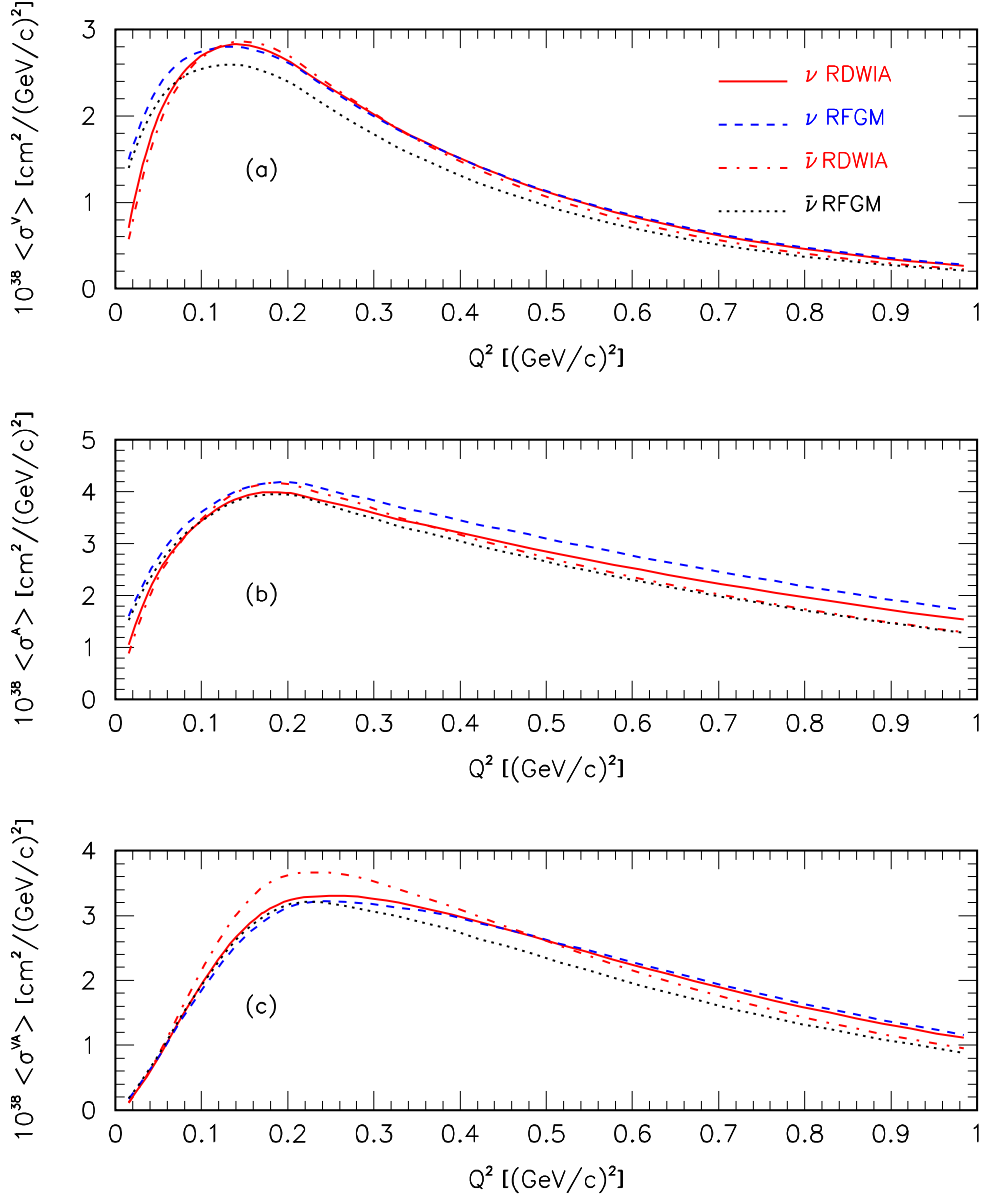
FIG. 2: (Color online) Flux-integrated $\langle \sigma^V \rangle^{\nu,\bar{\nu}}$, $\langle \sigma^A \rangle^{\nu,\bar{\nu}}$, and $\langle \sigma^{VA} \rangle^{\nu,\bar{\nu}}$ cross sections as functions of four-momentum transfer Q^2. As shown in the key, the cross sections were calculated in the RDWIA and RFGM with BNB ν_μ and $\bar{\nu}_\mu$ fluxes.

line (BNB) ν_μ and $\bar{\nu}_\mu$ fluxes. In Fig. 2 these cross sections, calculated within the RDWIA and RFGM (with the Fermi momentum $p_F = 221$ MeV/c and a binding energy $\epsilon_b = 25$ MeV for carbon), are shown as functions of Q^2. In the region $Q^2 \leq 0.25 (\text{GeV/c})^2$, the Fermi gas model results are higher than those obtained within the RDWIA. At $Q^2 \leq 0.05 (\text{GeV/c})^2$ this discrepancy equals $\sim 10\%$ for $\langle \sigma^V \rangle$, $\sim 12\%$ for $\langle \sigma^A \rangle$, and $\sim 8\%$ for $\langle \sigma^{VA} \rangle$. To extract

values for the axial form factor we calculated $\langle \sigma^i \rangle$ $(i = V, A, VA)$ cross sections with the BNB flux using the Q^2 bins $\Delta Q^2 = Q^2_{i+1} - Q^2_i$ similar to Refs. [2, 3]

$$\langle \sigma^i \rangle_j = \frac{1}{\Delta Q^2} \int_{Q^2_j}^{Q^2_{j+1}} \langle \sigma^i(Q^2) \rangle dQ^2 \qquad (18)$$

B. Extraction of the axial form factor

Flux-integrated $\langle d\sigma^\nu / dQ^2 \rangle$ and $\langle d\sigma^{\bar\nu} / dQ^2 \rangle$ cross sections for ν_μ and $\bar\nu_\mu$ CCQE scattering as functions of Q^2 together with the MiniBooNE data [2, 4] are shown in Figs. 3 and 4 (upper panel) correspondingly. The neutrino (antineutrino) cross section are scaled with the number of neutrons (protons) in the target. They are calculated in the RDWIA ($M_A = 1.37$ GeV) and RFGM ($M_A = 1.36$ GeV) approaches. Also shown in Figs. 3 and 4 are the normalized axial form factor $F_A(Q^2)/F_A(0)$ (lower panel) extracted within the RDWIA and Fermi gas model from the measured cross sections. The differences of the measured cross sections $\Delta[d\sigma/dQ^2] = \langle d\sigma/dQ^2 \rangle^\nu - \langle d\sigma/dQ^2 \rangle^{\bar\nu}$ are shown in Fig. 5 (upper panel) as a function of Q^2 compared with the RDWIA and RFGM calculations. Also shown are the normalized axial form factors extracted in these approaches from $\Delta[d\sigma/dQ^2]$ (lower panel). The total normalization error on the neutrino (antineutrino) cross section measurement is 10.7% (17.2%). To extract values of $F_A(Q^2)$ the measured cross sections with " the shape-only" error were used in Eq. (16).

There is an overall agreement between the calculated and measured neutrino cross sections across the full range of Q^2. The values of the normalized axial form factors extracted within the RDWIA are similar to the RFGM result. A good match between the dipole parametrization with $M_A = 1.37$ GeV and extracted form factors is observed. For antineutrino scattering there is an agreement between the calculated results and the data at $Q^2 \geq 0.1$ (GeV/c)^2 within the error of the experiment. However, the RDWIA result underestimates the measured cross section at $Q^2 < 0.1$ (GeV/c)^2. The values of $F_A(Q^2)$ extracted in the RDWIA and Fermi gas approaches at $Q^2 > 0.1$ (GeV/c)^2 also agree well with the dipole parametrization, whereas at $Q^2 \leq 0.1$ (GeV/c)^2 the RDWIA result is higher than the RFGM and dipole parametrization prediction. A good match between the calculated and measured differences $\Delta[d\sigma/dQ^2]$ is observed. The extracted axial form factors also agree well with the dipole approximation prediction with $M_A = 1.37$ GeV.
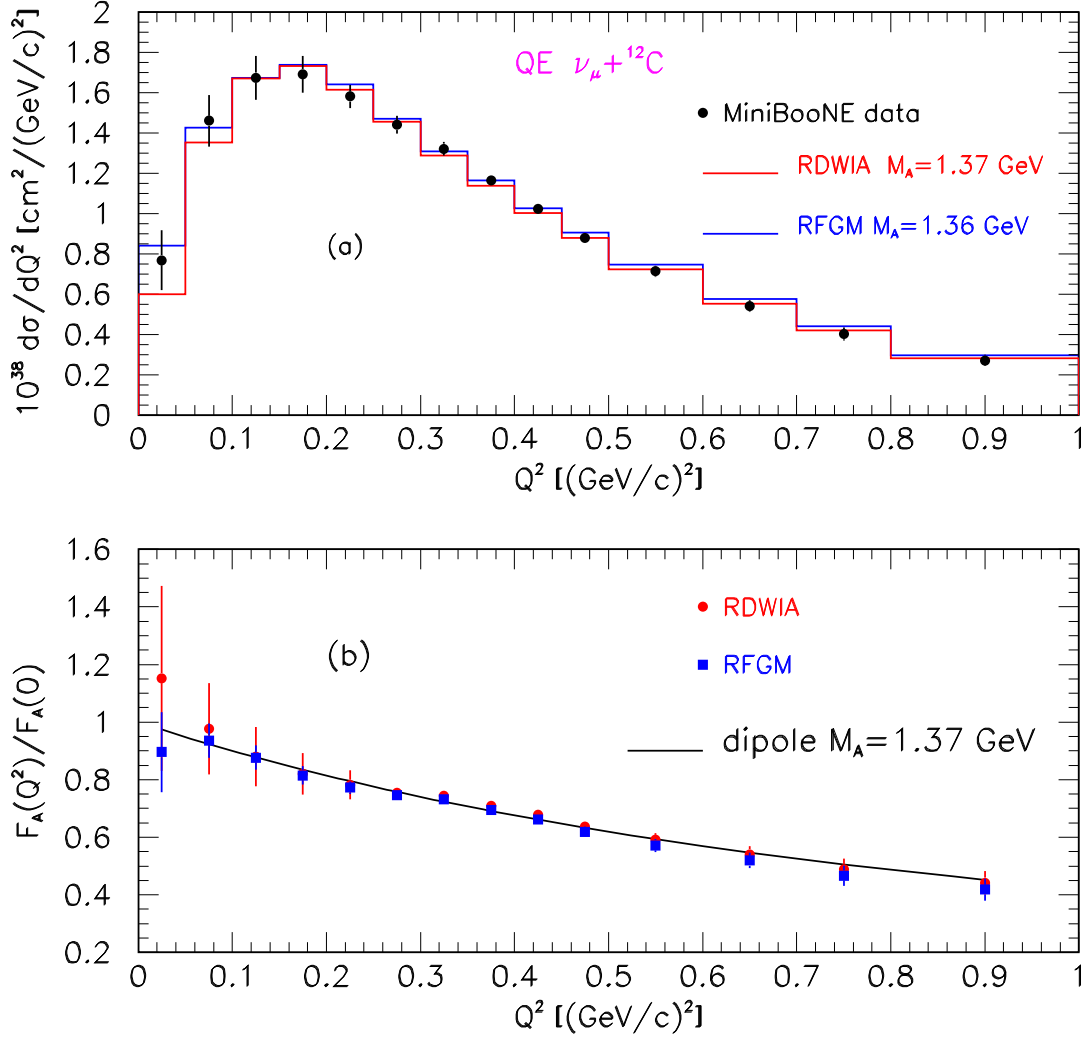
FIG. 3: (Color online) Flux-integrated $\langle d\sigma/dQ^2\rangle^\nu$ cross section per neutron target for the ν_μ CCQE scattering (upper panel) and the normalized axial form factor $F_A(Q^2)/F_A(0)$ extracted from the MiniBooNE data (lower panel). Upper panel: Calculations from the RDWIA with $M_A = 1.37$ GeV and RFGM with $M_A = 1.36$ GeV. Lower panel: Filled circles (filled squares) are the axial form factor extracted within the RDWIA (RFGM) and the solid line is the result of the dipole parametrization with $M_A = 1.37$ GeV.
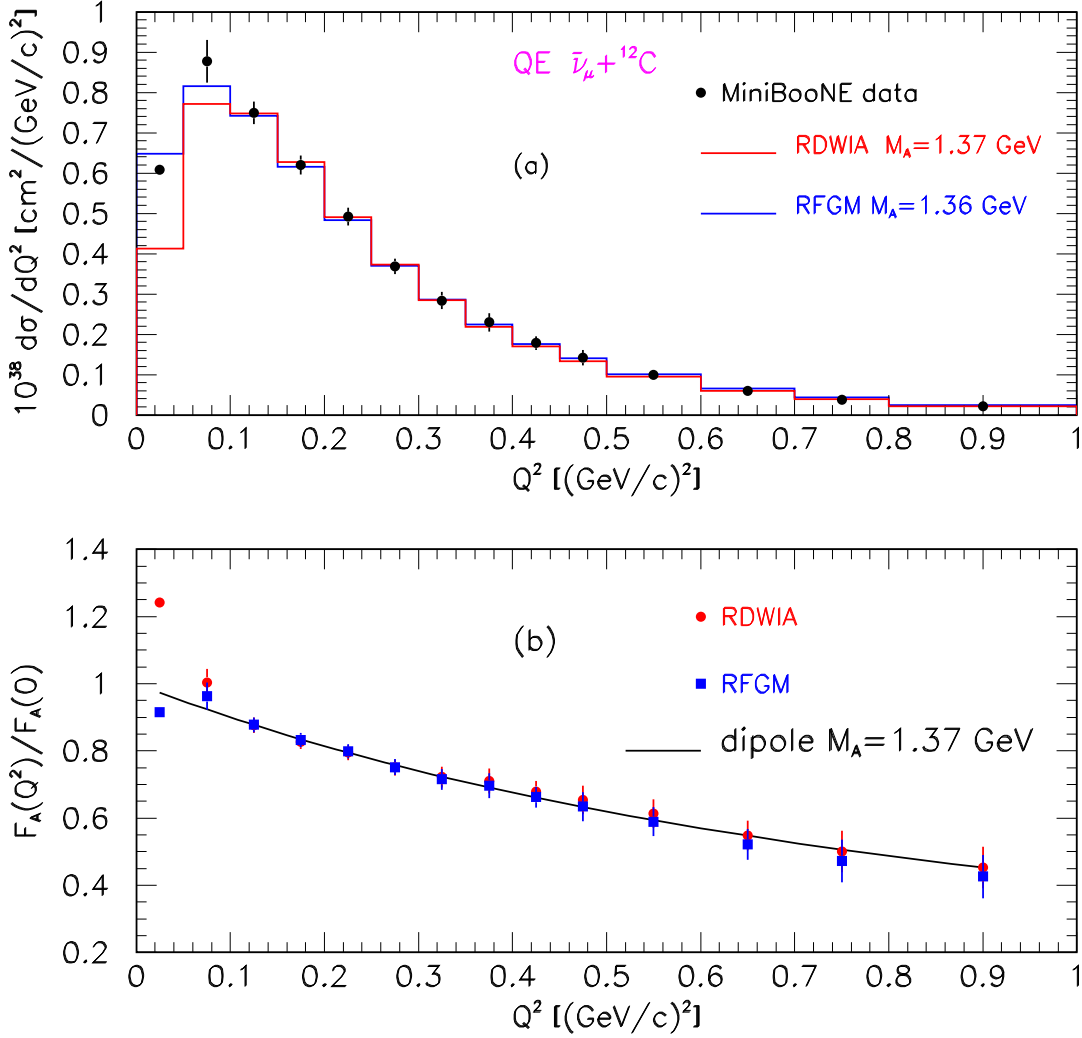
FIG. 4: (Color online) The same as Fig. 3, but for antineutrino scattering

In Ref. [28] it was assumed that enhancements in the transverse (anti)neutrino CCQE cross section are modified $F_M(Q^2)$, for a bound nucleon at low $Q^2 \approx 0.3$ (GeV/c)^2. The authors proposed a transverse enhancement function for the carbon target. If the TE originates from the MEC, then we may expect that enhancement in the longitudinal or axial contributions is small. Therefore in the TE model $F_V(Q^2)$ and $F_A(Q^2)$ are the same as for free nucleons. This approach was proposed to explain the apparent discrepancy between the low-(MiniBooNE) and high-(NOMAD) energy (anti)neutrino CCQE cross sections and M_A
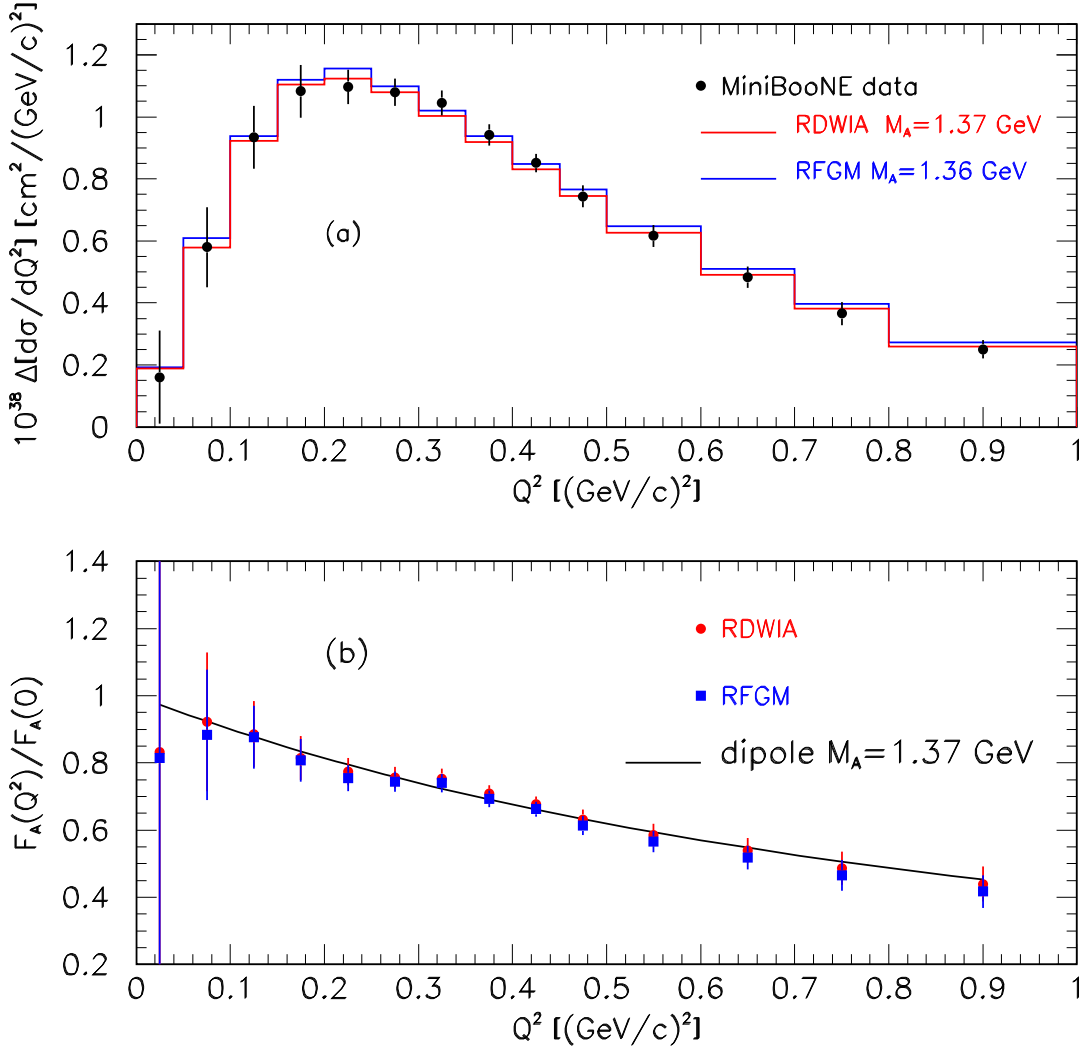
FIG. 5: (Color online) The same as Fig. 3 but for a difference of the measured cross sections $\Delta[d\sigma/dQ^2]$.

measurements.

To study the TE effects on the extracted axial form factor we compare results of the RFGM ($M_A = 1.36$ GeV) and the Fermi gas model ($M_A = 1.014$ GeV) with the transverse enhancement function from Ref. [28]. We call the last approach the RFGM + TE model [50]. The flux-integrated cross sections $\langle d\sigma^\nu/dQ^2 \rangle$ scaled with a number of neutron per target as functions of Q^2 together with the MiniBooNE data [2] are shown in Fig. 6. The upper

panel shows cross sections calculated in the RFGM and RFGM+TE models. Also shown in Fig. 6 (lower panel) are normalized axial form factors extracted in these approaches from measured cross section.

In the range $Q^2 \leq 0.5$ (GeV/c)^2 the differential cross section $\langle d\sigma^\nu/dQ^2 \rangle$ calculated within the RFGM+TE model is in agreement with the Fermi gas model prediction. However, in the region $Q^2 \geq 0.7$ (GeV/c)^2 the RFGM+TE result is lower than the measured cross section. Therefore, there is a disagreement between the form factors extracted in this approach and predicted by the dipole parametrization with $M_A = 1.014$ GeV. In the region $Q^2 \approx 0.2 - 0.3$ (GeV/c)^2 where an enhancement in the $F_M(Q^2)$ was assumed, the extracted values of F_A are lower than those predicted from the dipole approximation. At $Q^2 > 0.6$ (GeV/c)^2 the enhancement function disappears with higher values of Q^2 and the value of F_A extracted in the RFGM+TE model start approaching those extracted from the RFGM. As shown in Fig. 6 the shape of the Q^2 dependence of the axial form factor extracted within the RFGM+TE approach cannot be well described by the dipole ansatz. So, assuming the dipole parametrization of $F_A(Q^2)$ the MiniBooNE data may be described within the impulse approximation with large axial mass value ~ 1.3 GeV as well as within the approaches that include sizable MEC and IC contributions and allow reproduction of data with $M_A \sim 1$ GeV. But for the self-consistent description of the MiniBooNE data with the enhancement in the transverse response function (at least as it was proposed in Ref. [28]), one should use a parametrization of $F_A(Q^2)$ other than a dipole.

As was pointed in Ref. [31], the dipole approximation cannot be justified from a field-theoretic point of view and is in contradiction with the large-N_c-motivated parametrization. We calculated the normalized axial form factor by using the minimum meson-dominance ansatz from Ref.[31]:

$$F_A(Q^2) = F_A(0) \frac{m_{a_1}^2 m_{a_1'}^2}{(m_{a_1}^2 + Q^2)(m_{a_1'}^2 + Q^2)}, \tag{19}$$

where $m_{a_1} = 1.230$ GeV, and $m_{a_1'} = 1.647$ GeV. By applying the half-width rule $m_R \pm \Gamma_R/2$ to this parametrization with $\Gamma_{a_1} = 0.425$ GeV and $\Gamma_{a_1'} = 0.254$ GeV, we get results depicted in Fig. 7. The errors in the meson-dominanted form factor (the band for the form factor) are estimated by treating resonance masses as random variables distributed with the dispersion given by the width. As we can see, the agreement between the extracted form factor and the meson dominance ansatz is impressive. Actually, the two axial mesons are incorporated as a
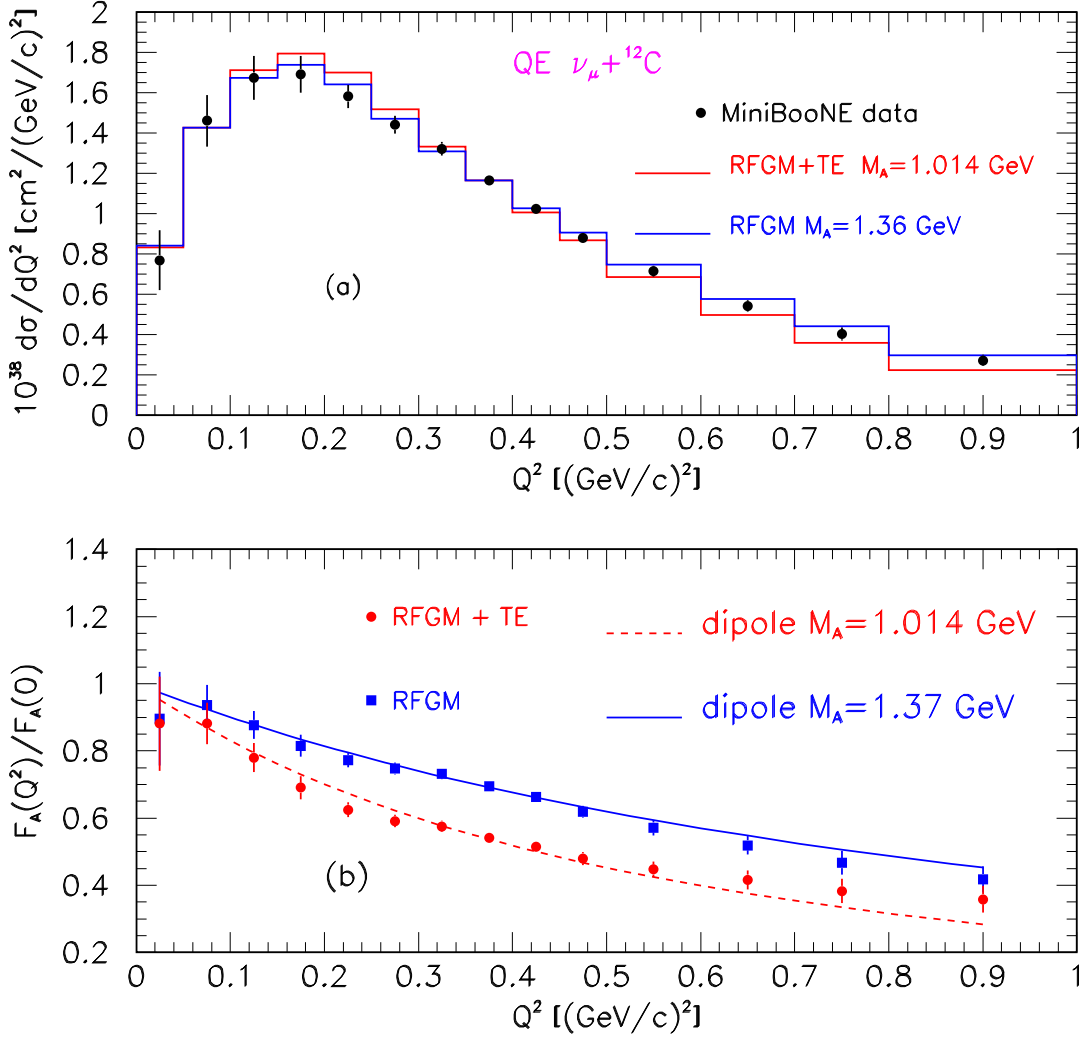
FIG. 6: (Color online) The same as Fig. 3, but calculated $\langle d\sigma^\nu/dQ^2 \rangle$ cross sections per neutron target and extracted form factors are from the RFGM ($M_A = 1.36$ GeV) and RFGM+TE ($M_A = 1.014$ GeV)

product of monopoles, but the net effect is essentially a dipole form factor with an average mass which is larger than $m_R = 1$ GeV.
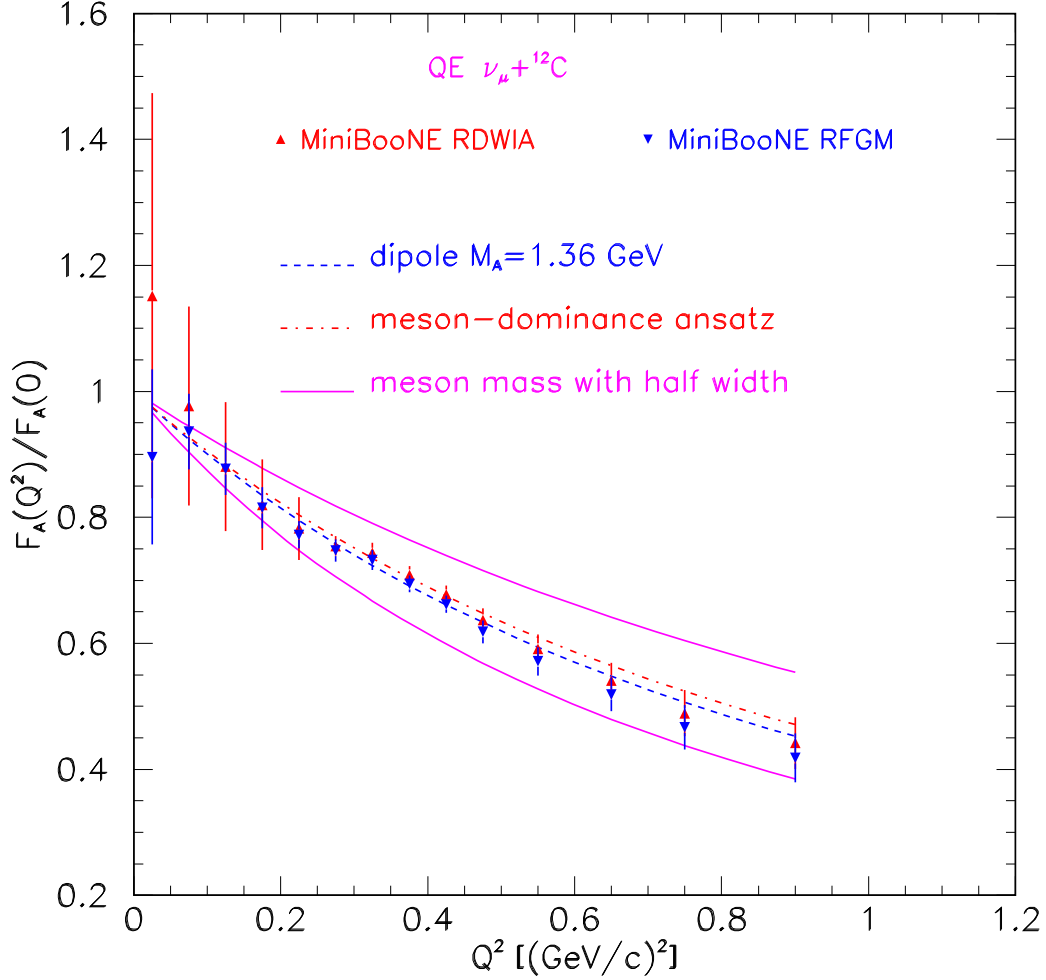
FIG. 7: (Color online) The normalized axial form factor $F_A(Q^2)/F_A(0)$ extracted from MiniBooNE data. The dashed line is the result of the dipole parametrization with $M_A = 1.36$ GeV, dashed-dotted line is the result of the meson-dominance ansatz, and solid lines show the bands for the form factor due to the half-width of the meson masses.

C. CCQE total cross section

We calculated the total cross sections for CCQE antineutrino scattering on carbon in the plane-wave impulse approximation (PWIA), RDWIA, and RFGM approaches. The cross section per proton target as a function of antineutrino energy is shown in Fig. 8 (lower
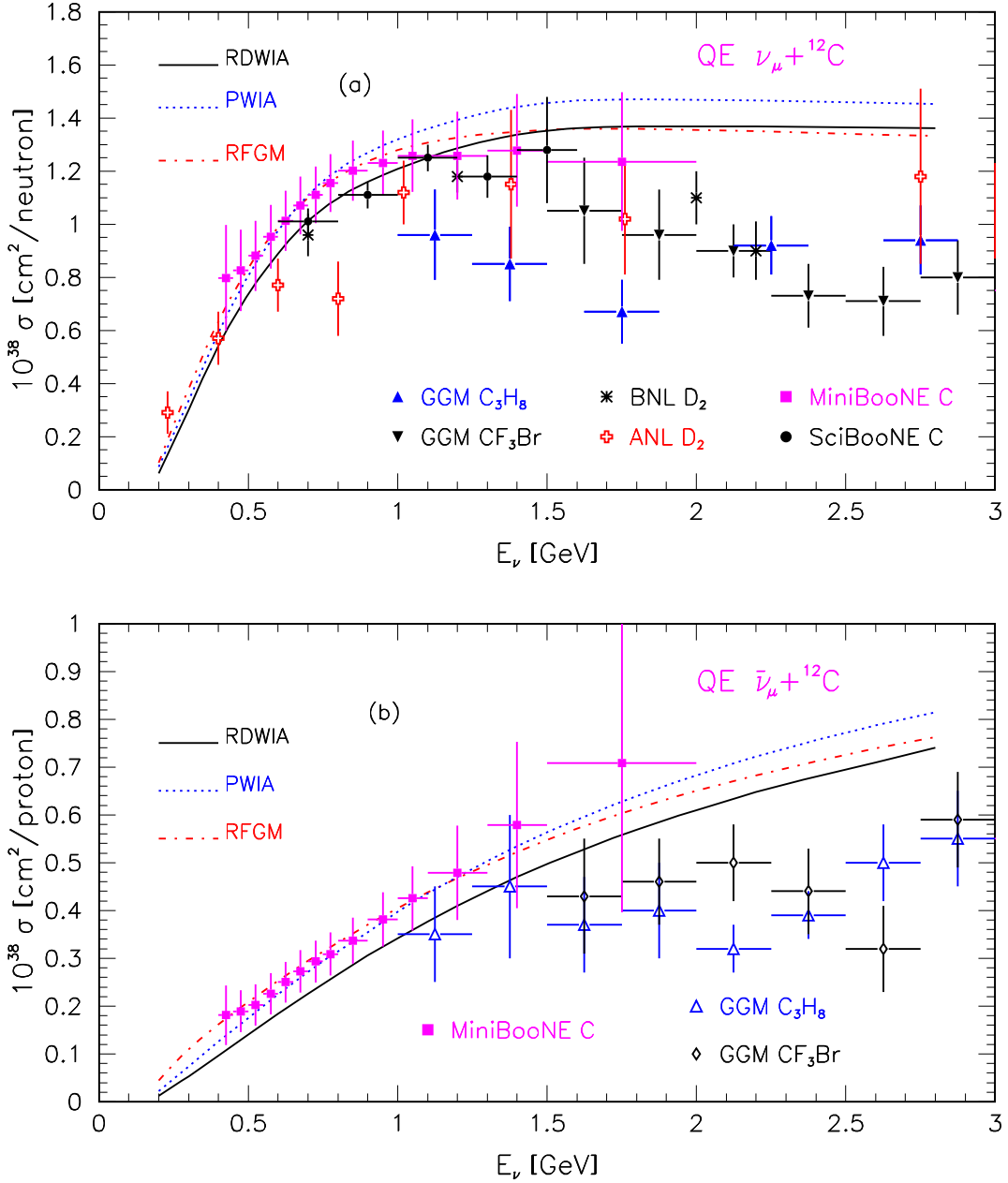
FIG. 8: (Color online) Total $\nu_\mu(\bar{\nu}_\mu)$ CCQE cross section per neutron (proton) target as a function of neutrino energy. Data points for different targets are from Refs. [3, 8, 51–54]. Also shown are predictions of the RDWIA ($M_A = 1.37$ GeV), PWIA ($M_A = 1.37$ GeV), and RFGM ($M_A = 1.36$ GeV).

panel) together with the data from Refs. [2, 4, 51–54]. Also shown are (upper panel) the total cross sections per neutron target for neutrino scattering from Ref. [17]. The calculated cross sections, which use the values of M_A extracted from the shape-only fit to the flux-integrated $d\sigma^{\nu,\,\bar{\nu}}/Q^2$ data, reproduce the MiniBooNE total cross section within the errors. At the energy of $\varepsilon_\nu \approx 700$ MeV, the extracted cross section is $\approx 30\%$ higher than what is commonly assumed for this process assuming the RFGM and world-average value of the axial mass $M_A = 1.03$ GeV. As shown in Fig. 7 the spread in the data is much higher than the difference in predictions of the RDWIA, PWIA, and RFGM approaches.

IV. CONCLUSIONS

In this paper, we present a method which allows extraction of the axial form factor as a function of Q^2 from flux-integrated $\langle d\sigma^{\nu,\bar{\nu}}/dQ^2 \rangle$ cross sections. This method is based on the fact that the $d\sigma/dQ^2$ can be written as the sum of the vector, axial and vector-axial cross sections and the contributions of the axial and vector-axial ones are proportional to $F_A^2(Q^2)$ and $F_A(Q^2)$ correspondingly. In our analysis we used the differential $\langle d\sigma^{\nu,\bar{\nu}}/dQ^2 \rangle$ CCQE cross sections with "a shape-only" error measured in the MiniBooNE experiment.

In the RDWIA, RFGM, and RFGM+TE approaches with the BNB $\nu_\mu(\bar{\nu}_\mu)$ flux we calculated the flux-integrated vector, axial, and vector-axial cross sections which were used for extraction of the axial form factor. The values of $F_A(Q^2)$ extracted in the RDWIA and Fermi gas models at $Q^2 > 0.1$ (GeV/c)^2 agree well with the dipole parametrization with $M_A \approx 1.37$ GeV. On the other hand the vector meson-dominance ansatz that is simple and has good theoretical base describes the extracted form factor also with a good agreement. We can argue that there is no need to use the dipole approximation for fitting the MiniBooNE data and that the meson dominance already contains the essential physical information, whereas we found that there is a disagreement between the form factors extracted in the RFGM+TE approach and predicted by the dipole approximation with $M_A \approx 1.04$ GeV. The RDWIA, PWIA and RFGM calculated with $M_A = 1.37$ GeV and measured neutrino and antineutrino CCQE total cross sections match well within the experimental error over the entire measured range.

We conclude that the MiniBooNE measured inclusive and total cross sections can be described within the impulse approximation with the meson-dominance ansatz and/or dipole

approximation of $F_A(Q^2)$ with large axial mass value. In addition, one could also describe MiniBooNE data with the approach that incorporates the large MEC contributions. However, a non-dipole description of the axial from factor would have to be used in that case. From the quality of the fit to the measured MiniBooNE CCQE cross section, one could not discriminate between these approaches.

So, to distinguish between various possible mechanisms, it is necessary to decompose the inclusive process into its constituents exclusive channels, at least to study the semiexclusive $\nu_\mu + A \to \mu + p + B$ process. In this manner one hopes to disentangle the roles of NN correlations in the target ground state, MEC, IC, medium modifications properties of the bound nucleon, many-body currents, FSI, relativistic corrections et cetera, etc. [55]

Acknowledgments

[1] V. Lyubushkin *et al.*, (NOMAD Collaboration), Eur. Phys. J. **C63**, 355, (2009).

[2] A. A. Aguilar-Arevalo *et al.*, (MiniBooNE Collaboration), Phys. Rev. **D81**, 092005 (2010).

[3] A. A. Aguilar-Arevalo *et al.*, (MiniBooNE Collaboration), Phys. Rev. **D82**, 092005 (2010).

[4] A. A. Aguilar-Arevalo *et al.* (MiniBooNE Collaboration) Phys. Rev. **D88**, 032001 (2013).

[5] L. Fields *et al.*, (MINERvA Collaboration), Phys. Rev. Lett. **111**, 022501 (2013).

[6] G. A. Fiorentini *et al.*, (MINERvA Collaboration), Phys. Rev. Lett. **111**, 022502 (2013).

[7] K. Abe *et al.*, (T2K Collaboration), Phys. Rev. **D87**, 092003 (2013).

[8] Y. Nakajima *et al.*, (SciBooNE Collaboration), Phys. Rev. **D83**, 012005 (2011).

[9] R. A. Smith and E. J. Moniz, Nucl. Phys.**B43**, 605 (1972); *erratum: ibid.* **B101**, 547 (1975).

[10] V. Bernard, L. E. Elouadrhiri, U. -G. Meissner J. Phys. **G28**, R1, (2002).

[11] R. Gran *et al.*, (K2K Collaboration), Phys. Rev. **D74**, 052002 (2006).

[12] X. Espinal, F. Sanchez, AIP (Conf. Proc.) **967**, 117 (2007).

[13] M. Dorman *et al.* (MINOS Collaboration), AIP Conf. Proc. **1189**, 133 (2009).

[14] N. S. Mayer, PhD Thesis, Indiana Univ. (2011).

[15] O. Benhar, P. Coletti, and D. Meloni, Phys. Rev. Lett.**105**, 132301 (2010).

[16] C. Juszczak, J. T. Sobczyk, and J. Zmuda, Phys. Rev. **C82**, 045502 (2010).

[17] A. V. Butkevich, Phys. Rev. **C82**, 055501 (2010).

[18] A. V. Butkevich, and D. Perevalov, Phys. Rev. **C84**, 015501 (2011).

[19] A. Meucci, C. Giusti, Phys. Rev. **D85**, 093002 (2012).

[20] M. Martini, M. Ericson, G. Chanfray, and J. Marteau, Phys. Rev. **C81**, 045502 (2010)

[21] M. Martini, M. Ericson, and G. Chanfray, Phys. Rev. **C84**, 055502 (2011)

[22] J. Nieves, I. R. Simo and M. J. Vicente Vacas, Phys. Rev. **C83**, 045501 (2011).

[23] J. Nieves, I. Ruiz Simo, and M. J. Vicente Vacas, Phys. Lett. **B707**, 72 (2012).

[24] J. Nieves, I. Ruiz Simo, and M. J. Vicente Vacas, Phys. Lett. **B721**, 90 (2013).

[25] J. E. Amaro, M. B. Barbaro, J. A. Caballero, T. W. Donnelly, and C. F. Williamson, Phys. Lett. **B696**, 151 (2011).

[26] J. E. Amaro, M. B. Barbaro, J. A. Caballero, T. W. Donnelly, J. M. Udias, Phys. Rev. **D84**, 033004 (2011).

[27] J. E. Amaro, M. B. Barbaro, J. A. Caballero, T. W. Donnelly, Phys. Rev. Lett. **108**, 152501 (2012).

[28] A. Bodek, H. Budd, and M. Christy, Eur. Phys. J. **C71**, 1, (2011).

[29] O. Lalakulich, K. Gallmeister, and U. Mosel, Phys. Rev. **C86**, 014614, (2012).

[30] B. Bhattacharya, R. J. Hill, and G. Paz, Phys. Rev. **D84**, 073006 (2011).

[31] P. Masjuan, E. R. Arriola, and W. Broniowski, Phys. Rev. **D87**, 014005 (2013).

[32] A. Bodek, S. Avvakumov, R. Bradford, and H. Budd, Eur. Phys. J. **C53**, 349, (2008).

[33] A. V. Butkevich and S. A. Kulagin, Phys. Rev. **C76**, 045502 (2007).

[34] A. V. Butkevich, Phys. Rev. **C78**, 015501 (2008).

[35] A. V. Butkevich, Phys. Rev. **C80**, 014610 (2009).

[36] A. V. Butkevich, Phys. Rev. **C85**, 065501 (2012).

[37] P. Mergell, U.-G. Meissner, and D. Drechesel, Nucl. Phys. **A596**, 367, 1996.

[38] T. de Forest, Nucl. Phys. **A392**, 232, 1983.

[39] B. Serot, J. Walecka, Adv. Nucl. Phys. **16**, 1, 1986.

[40] C. J. Horowitz D. P. Murdock, and Brian D. Serot, in *Computational Nuclear Physics 1: Nuclear Structure* edited by K. Langanke, J. A. Maruhn, Steven E. Koonin (Springer-

Verlag,Berlin, 1991), p.129

[41] D. Dutta *et al.*, Phys. Rev. **C68**, 064603, (2003).

[42] J. J. Kelly Phys. Rev. **C71**, 064610 (2005).

[43] D. Rohe *et al.*, Nucl. Phys. B (Proc. Suppl.) **159**, 152 (2006).

[44] J. J Kelly, http://www.physics.umd.edu/enp/jjkelly/LEA

[45] E .D. Cooper, S. Hama, B. C. Clark, and R. L. Mercer, Phys. Rev. **C47**, 297 (1993).

[46] K. G. Fissum *et al.*, Phys. Rev. **C70**, 034606, 2004

[47] C. H. Llewellyn Smith, Phys. Rep. **3C**, 1, 1972

[48] H. Budd, A. Bodek, and J. Arrington, Nucl. Phys. B. (Proc. Suppl) **139**, 90, (2005).

[49] A. A. Aguilar-Arevalo *et al.*, (MiniBooNE Collaboration), Phys. Rev. **D79**, 072002 (2009).

[50] J. T. Sobczyk, Eur. Phys. J. **C72**, 1850 (2012).

[51] W. A. Mann *et al.*, Phys. Rev. Lett. **31**, 844, (1973).

[52] N. J. Baker *et al.*, Phys. Rev. **D23**, 2499, (1981).

[53] M. Pohl *et al.*, Lett. Nuovo Cim. **26**, 332, 1979.

[54] J. Brunner *et al.*, Z. Phys. **C45**, 551, 1990.

[55] J. J. Kelly, Adv. Nucl. Phys. **23**, 75, 1996